Ann Med Res

Current issue list available at Ann Med Res

Annals of Medical Research

journal page: annalsmedres.org

Evaluating peripapillary choroidal vascularity index and peripapillary retinal nerve fiber layer thickness in patients with retrobulbar optic neuritis: A comparative study

Hidayet Sener [a],*, Hatice Kubra Sonmez [a]

[a]Erciyes University, Faculty of Medicine, Department of Ophthalmology, Kayseri, Türkiye
*Corresponding author: hidayetsener00@gmail.com (Hidayet Sener)

MAIN POINTS

- The posterior tibial curvature is significantly greater in the proximal region than in the distal region.
- Understanding tibial curvature is essential for accurate surgical planning and avoiding postoperative complications.
- This study presents a practical morphometric method for evaluating posterior tibial curvature on the sagittal plane.

Cite this article as: Sener H, Sonmez HK. Evaluating peripapillary choroidal vascularity index and peripapillary retinal nerve fiber layer thickness in patients with retrobulbar optic neuritis: A comparative study. *Ann Med Res*. 2025;32(5):210–216. doi: 10.5455/annalsmedres.2025.01.02.

ABSTRACT

Aim: This study aimed to determine whether the peripapillary choroidal vascular index (pCVI) can be used to diagnose and track retrobulbar optic neuritis (RBON) and to compare the clinical and electrophysiological characteristics between patients with RBON and controls.

Materials and Methods: The study involved 60 eyes, and evaluations included magnetic resonance imaging (MRI), optical coherence tomography (OCT), visual field (VF) testing, and pattern visual-evoked potential (VEP) testing.

Results: Twenty eyes with RBON, twenty fellow eyes, and twenty healthy control eyes were enrolled. Age, gender, and axial length were not significantly different between the groups. Best-corrected visual acuity (BCVA) was substantially lower in RBON eyes than in both fellow and control eyes ($p<0.0167$). The peripapillary choroidal vascular index (pCVI) was also significantly reduced in the RBON eyes compared with the control eyes ($p<0.001$). Although RBON eyes showed longer P100 latency ($p = 0.019$) and reduced temporal peripapillary retinal nerve fiber layer (pRNFL) thickness ($p = 0.045$), these differences did not reach statistical significance.

Conclusion: Our findings demonstrate a reduction in pCVI and visual acuity in RBON eyes compared with controls, suggesting a potential role of vascular dysfunction in the disease process. Although other structural and electrophysiological changes were observed, they did not remain statistically significant.

Keywords: Optic neuritis, Choroidal vascularity index, Retinal nerve fiber layer, Visual evoked potential, Visual field

Received: Jan 02, 2025 **Accepted:** Apr 21, 2025 **Available Online:** May 26, 2025

INTRODUCTION

Retrobulbar optic neuritis (RBON), an inflammatory demyelinating disease that the optic nerve, is commonly associated with multiple sclerosis (MS) and neuromyelitis optica [1,2]. This disorder affects the part of the optic nerve behind the eye, resulting in visual abnormalities, such as color vision, blurred vision, and visual field deficiency [3]. Ongoing advances in imaging technology have led to an unprecedented increase in the detailed visualization of ocular structures, with a particular focus on the choroidal vasculature [4]. The choroid, a critical supplier of blood to the outer retina, is increasingly recognized for its role in several ocular pathologies [5].

The peripapillary choroidal vascular index (pCVI), which quantifies choroidal vessel density around the optic nerve head (ONH), has emerged as a promising tool for assessing optic nerve health [6]. However, studies evaluating the potential of pCVI for the diagnosis and monitoring of RBON are lacking.

This study aimed to investigate clinical and electrophysiological characteristics in patients with RBON and compare them to controls. The study also evaluated visual field (VF) outcomes, visual-evoked potential (VEP) tests, and changes in the retinal nerve fiber layer (RNFL) and pCVI among patients with RBON. This approach would help enhance our understanding of the disease's impact on optic nerve health and the potential role of choroidal vasculature in RBON.

MATERIALS AND METHODS

All methods employed in this research involving human participants strictly followed the ethical norms of the Helsinki Declaration. The research protocol received approval from the Institutional Review for ethical scientific conduct (Erciyes University Local Ethics Committee, No:2023/39).

Study population

This study included patients who presented with acute vision loss and were subsequently diagnosed with RBON at our institution. Comparisons were conducted between the affected eye and the healthy fellow eye of each patient, as well as with a randomly selected eye of a healthy patient attending the clinic. We excluded patients with a history of other ophthalmologic or neurologic diseases that could potentially influence the optic nerve, individuals with a medical history of bilateral retrobulbar neuritis, papillitis, and ischemic optic neuropathy, and those with pre-existing conditions such as diabetes or hypertension. Pediatric patients were also not included in this research. In patients diagnosed with RBON, images were obtained at least 3 months after the acute attack.

Clinical examination

All patients underwent a thorough ophthalmologic examination upon presentation, which included a dilated funduscopic examination, intraocular pressure (IOP) measurement, slit-lamp examination, and best-corrected visual acuity (BCVA) assessment. Relative afferent pupillary deficit (RAPD) was noted, and any aberrant findings were recorded.

Optical Coherence Tomography (OCT)

An ONH radial circle scan pattern and 24 continuous radial B-scans were obtained using the Spectralis OCT Glaucoma Module software (version 1.9.17.0; Heidelberg Engineering). The structures are arranged according to the axis running from the fovea to the Bruch's Membrane Opening (BMO) center. Every location along a predefined-diameter (3.5 mm) circle in a comprehensive area, as well as in the six different sectors, was used to calculate the thickness of the RNFL in the circumpapillary region (Figure 1).

VF test

We used the Octopus 900 perimeter (Haag-Streit, Switzerland) to perform the VF tests on our study participants. The VF test uses the 30-2 white/white pattern. Each subject was comfortably seated, and the test was performed in a dimly lit room. The nontested eye was occluded, and patients were instructed to fixate on the central target throughout the test. False-positive and false-negative responses and fixation losses were carefully recorded during the test to assess the reliability of the test results. Mean deviation (MD) is a measure quantifying the overall reduction or defect in a patient's visual field (VF) relative to the normal visual field of individuals in their age group. sLV measures the degree of localized VF loss.

Pattern VEP test

The VEP recordings were performed using the Vision Monitor by Metrovision (MonPack, France). This study was performed following the recommended standard protocol by the International Society for Clinical Electrophysiology of Vision (ISCEV) [7]. A thorough explanation of the process was provided to each patient, and measures were taken to optimize their visual acuity. The active electrode was positioned on the visual cortex (Oz region as per the international 10-20 system), the reference electrode was positioned on the midfrontal head region (Fz region), and the ground electrode was placed on the mastoid.

We employed a reversed checkerboard pattern as the stimulus. The chosen field size was 15 minutes of visual arc. The contrast level was kept equal to or above 85%, with an average luminance of approximately 100 cd/m^2. The temporal frequency was set at 2 pattern reversals per second (1Hz). The patient was situated a meter away from the screen. The patients' pupils were nondilated under ambient room illumination. The participants were instructed to maintain steady fixation at the center of the stimulus field. Needle electrodes were used. The recording time window was set for 250 milliseconds, with at least 100 sweeps averaged for each response. Furthermore, the bandpass was set at 1-30 Hz.

We measured the implicit time and amplitude of the positive wave at approximately 100 ms (P100) and the negative wave at approximately 75 ms (N75). The P100 amplitude was measured from the N75 trough to the next peak, while the N75 amplitude was calculated from the baseline to the negative trough. The time between the beginning of light and the peak of the waves is known as the implicit time.

Magnetic Resonance Imaging (MRI), diagnosis, and treatment

Patients with RBON based on clinical examination were referred for neuroimaging. The MRI of the craniocervical and orbital region with gadolinium was performed to confirm the diagnosis. The diagnosis of RBON is based on a combination of clinical findings, such as sudden unilateral visual loss, the presence of RAPD and color vision loss, and a combination of test results of prolonged VEP implicit time and VF defects. Patients diagnosed with RBON were treated with a pulse prednisolone (Prednol-L, Gensenta, Turkey) therapy of 1g, administered over a period of 3–5 days.

OCT image processing procedure

The Choroidal Vascularity Index (CVI) was assessed using a 3.5-mm ONH radial circle scan, facilitated by the Spectralis Glaucoma Module software. Further information on the method used to measure CVI can be found in other sources [8–10]. Image binarization, the process of converting grayscale images to binary images, was performed using ImageJ software (version 1.47, available freely at https://imagej.net/Citing).

https://doi.org/10.5455/annalsmedres.2025.01.02

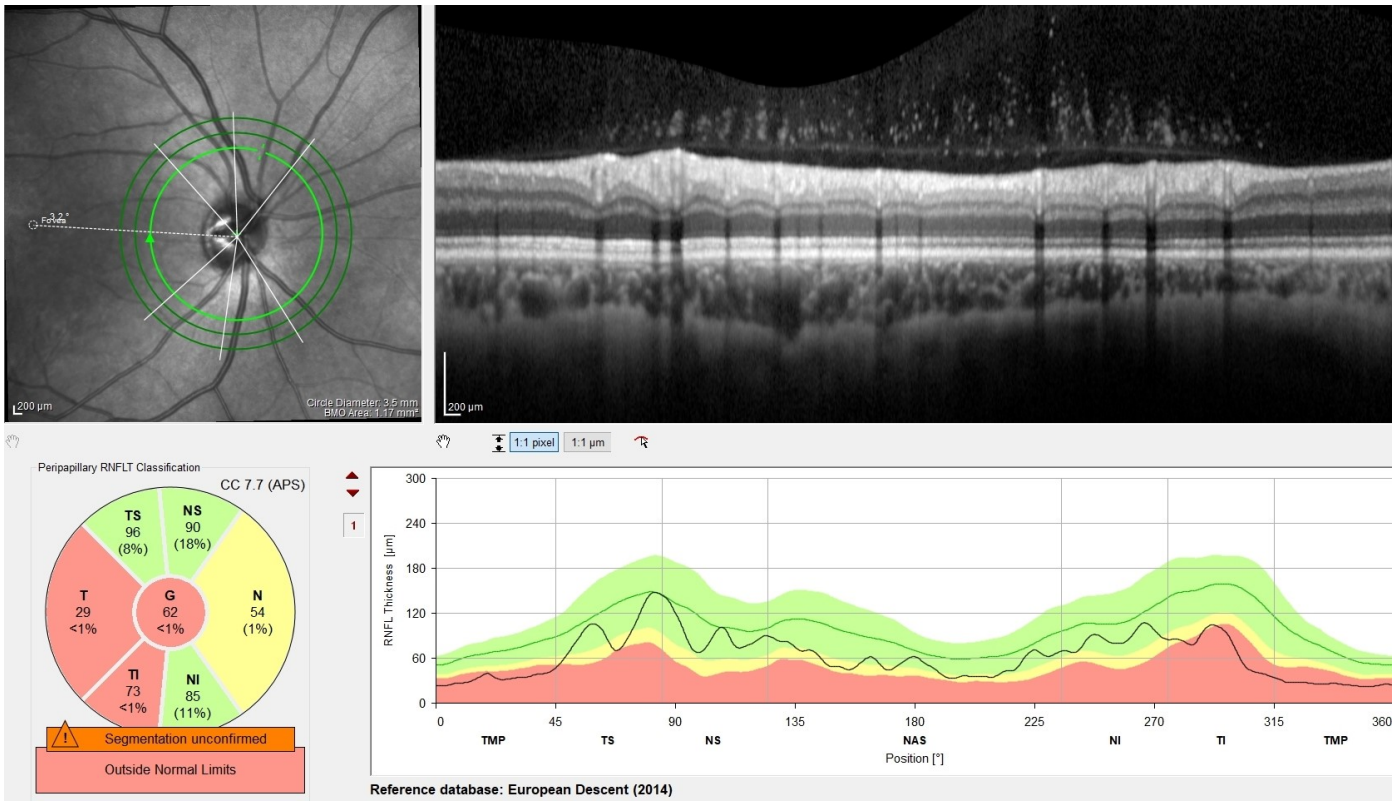

Figure 1. This figure shows the patient's SPECTRALIS Glaucoma Module scans with circumpapillary RNFL and optic disc imaging. The 3.5-mm RNFL scan results were obtained using the TSNIT profile and 6-sector analysis.

The area between the upper boundary of the light pixels at the Retinal Pigment Epithelium (RPE) and the lower boundary at the choroid-scleral junction was determined to be the choroidal area. The Total Choroidal Area (TCA), which is the area between the RPE and the choroid-scleral junction, was calculated after the picture color was changed to yellow so that the color threshold tool could detect dark pixels. The vascular region of dark pixels inside the choroid was identified as the Luminal Area (LA). Next, the LA was divided by the TCA to determine the pCVI (Figure 2).

Statistical analysis

All statistical analyses were performed using Statistical software Package for Social Sciences version 22 (SPSS version 22.0) (IBM Corp., Armonk, NY, USA). Shapiro-Wilk test was used as the test of normality. Homogeneity of variances was assessed using Levene's test. Based on these tests, statistical differences between groups were evaluated using the relevant parametric or nonparametric test. The Pearson chi-square test was used to compare nominal data.

Non-normally distributed data were subjected to the Wilcoxon signed-rank test. The Student's t-test was used for normally distributed data, whereas the Mann–Whitney U test was used for data that was not for independent groups. The results are displayed as mean ± standard deviation (SD) for normally distributed data and as median and interquartile range (IQR: 25^{th} to 75^{th} percentile) for nonnormally distributed data.

Comparisons among the three groups (RBON eyes, fellow eyes, and control eyes) were performed using paired or independent t-tests, as appropriate. To control for type I errors caused by multiple comparisons, Bonferroni correction was used. The significance threshold was adjusted to $\alpha = 0.05/3 \approx 0.0167$.

A post-hoc power analysis was conducted using G*Power software (Heinrich-Heine-Universität Düsseldorf, Düsseldorf, Germany) to assess whether the sample size was sufficient to detect differences in the peripapillary choroidal vascularity index (pCVI) among the three groups. The analysis was based on a one-way ANOVA (fixed effects, omnibus), with an alpha level of 0.05, three groups, and an effect size (Cohen's f) derived from the observed means and standard deviations. The resulting statistical power and Type II error probability (β) were calculated accordingly.

RESULTS

Twenty eyes with RBON, twenty buddy eyes, and twenty healthy control eyes comprised the total number of eyes enrolled. The patient and control groups did not differ significantly in terms of sex (p=0.185) or age [patient group: 41.0 (26.0-43.7, control group: 28.0 (30.0-32.0); p=0.056]. Eyes with RBON, other eyes, and controls had comparable axial lengths. However, compared with the controls and other eyes, eyes with RBON showed a markedly lower BCVA (Table 1). Nine members of the RBON group had relapsing-remitting multiple sclerosis.

https://doi.org/10.5455/annalsmedres.2025.01.02

Table 1. Demographic and clinical characteristics of patients.

Variables	RBON eye (n=20)	Fellow eye (n=20)	Control eye (n=20)	p1	p2	p3
Age (year)	41.0 (26.0-43.7)		28.0 (30.0-32.0)		0.056	
Sex (m/f)	5/15		9/11		0.185	
BCVA (decimal)	0.95 (0.62-1.00)	1.00 (1.00-1.00)	1.00 (1.00-1.00)	**0.007***	**0.006***	0.289
Axial lenght (mm)	23.1±1.0	23.2±1.0	23.7±1.0	0.618	0.124	0.154

*BCVA: best-corrected visual acuity; p1: RBON eye v fellow eye; p2: RBON eye v control eye; p3: fellow eye v control eye, RBON: retrobulbar optic neuritis, *significant p value.*

Table 2. Electrophysiological tests results of patients with RBON.

Variables	RBON eye (n=20)	Fellow eye (n=20)	p
N75_IT (ms)	61.2 (38.0-77.3)	72.9 (45.5-78.4)	0.455
N75_A (mV)	1.3 (0.2-2.9)	0.5 (0.2-1.9)	0.130
P100_IT (ms)	115.3±13.5	104.6±9.3	0.019
P100_A (mV)	8.1±4.0	8.6±5.1	0.452
Visual Field (md)	6.1±4.	4.2±3.4	0.078
Visual Field (sLV)	6 4.9±2.1	4.1±1.8	0.051

*RBON: retrobulbar optic neuritis, *significant p value.*

Table 3. OCT test results of patients and controls.

Variables	RBON eye (n=20)	Fellow eye (n=20)	Control eye (n=20)	p1	p2	p3
pRNFL_T (µm)	59.8±18.8	64.9±15.7	69.6±9.3	0.154	0.045	0.259
pRNFL_IT (µm)	142.0±44.3	139.1±30.8	146.8±14.7	0.741	0.649	0.323
pRNFL_IN (µm)	107.1±25.8	103.3±21.7	106.0±18.4	0.434	0.878	0.625
pRNFL_N (µm)	79.1±19.6	75.5±22.1	84.5±14.2	0.348	0.330	0.135
pRNFL_SN (µm)	122.5±28.5	115.7±25.9	118.8±28.3	0.265	0.683	0.724
pRNFL_ST (µm)	119.1±33.7	118.6±25.7	132.7±23.0	0.928	0.145	0.323

*RBON: retrobulbar optic neuritis; RNFL: retinal nerve fibre layer; p1: RBON eye v fellow eye; p2: RBON eye v control eye; p3: fellow eye v control eye, *significant p value.*

Table 4. CVI results of patients and controls.

Variables	RBON eye (n=20)	Fellow eye (n=20)	Control eye (n=20)	p1	p2	p3
CVI (%)	67.9±2.3	68.3±1.3	69.8±3.3	0.323	0.042	0.070
TCA (mm^2)	4.1±1.2	4.0±0.9	2.3±0.5	0.469	**<0.001***	**<0.001***
LA (mm^2)	2.8±0.8	2.8±0.6	1.6±0.4	0.575	**<0.001***	**<0.001***
SA (mm^2)	1.3±0.5	1.3±0.3	0.7±0.2	0.338	**<0.001***	**<0.001***
LA/SA (%)	0.48±0.05	0.46±0.02	0.44±0.07	0.240	0.047	0.102

*CVI: choroidal vascularity index, TCA: total choroidal area, LA: luminal area, SA: stromal area, p1: RBON eye v fellow eye; p2: RBON eye v control eye; p3: fellow eye v control eye, *significant p value.*

The eyes with RBON and the other eyes were the only ones whose VEP and VF test results were compared. The amplitude of the P100 wave and the implicit timing and amplitude of the N75 wave did not significantly differ between the eyes with RBON and the other eyes. Although the eyes with RBON showed a longer implicit time for the P100 wave (p = 0.019), this difference did not reach statistical significance. There was no significant difference in visual field (VF) between eyes with RBON and control eyes (Table 2).

The RBON eye had a lower average peripapillary retinal nerve fiber layer thickness (pRNFL_T) than the control eye (59.8 µm vs. 69.6 µm), but the difference was not statistically significant (p = 0.045). The RBON, fellow, and control eyes did not differ significantly in average pRNFL thickness across different sectors (Table 3).

CVI of the eyes with RBON was significantly lower than that of the control eye (67.9% vs. 69.8%, p < 0.001); however, the difference between the RBON and fellow eyes (p = 0.042) did not reach statistical significance. TCA, LA, and SA of the eyes with RBON were significantly lower in comparison to the fel-

https://doi.org/10.5455/annalsmedres.2025.01.02

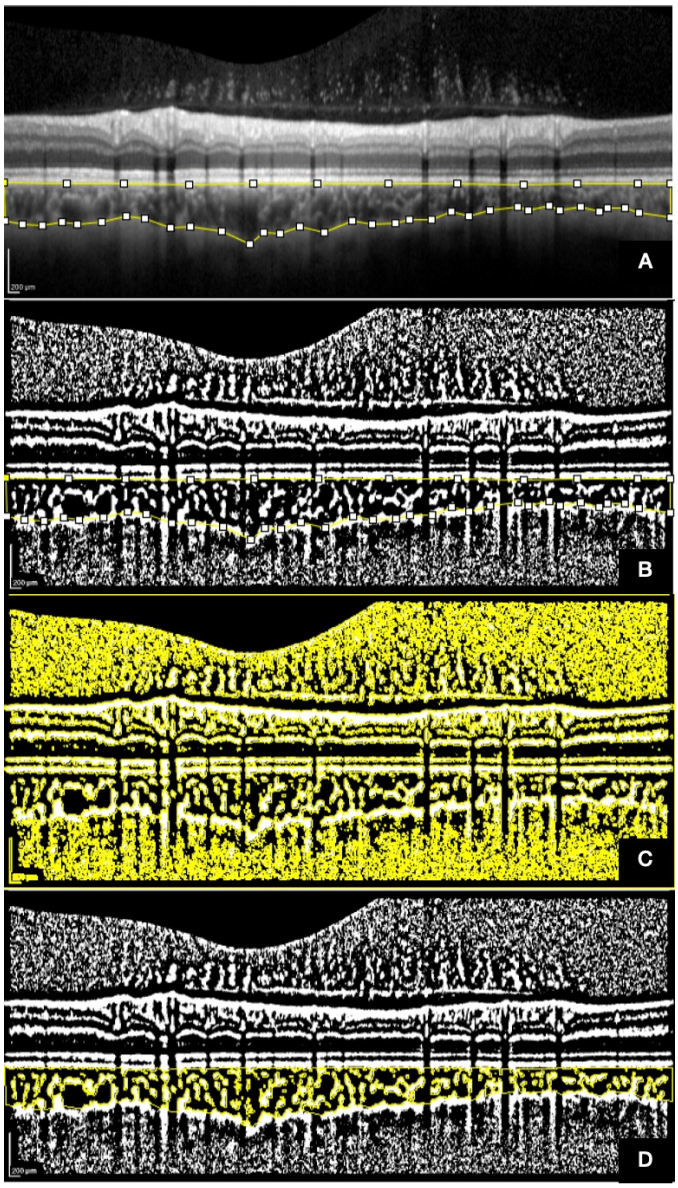

Figure 2. This sequence of images illustrates the process of image binarisation using ImageJ software. (A) The total peripapillary choroidal area was determined using the polygon tool in ImageJ software. (B) The image was then converted to an 8-bit image and autolocal thresholding was applied. (C) The Niblack method was selected to obtain a clear segmentation of the choroidal black and white areas. (D) Finally, the binarized image was converted back to an RGB image.

low normal eye (all p values < 0.001). The LA/SA ratio was lower in RBON eyes than in controls, but the difference was not statistically significant (Table 4).

A post-hoc power analysis was conducted to evaluate if the sample size was sufficient to detect group differences in pCVI. The mean pCVI values were 67.9% in RBON eyes, 68.3% in fellow eyes, and 69.8% in control eyes, with standard deviations of 2.3, 1.3, and 3.3, respectively. A one-way ANOVA was used to assess differences among the three groups. Based on these values, the calculated effect size (Cohen's f) was 0.44, indicating a moderate-to-large effect. With a sample size of 20 participants per group and a significance level (α) of 0.05, the probability of committing a Type II error (β) was approximately 0.155. Accordingly, the achieved statistical power was 84.5%, surpassing the conventional threshold of 80% required for adequate power. These findings suggest that the study was sufficiently powered to detect statistically significant differences in pCVI among groups, thereby reinforcing the robustness of the reported outcomes.

DISCUSSION

We aimed to elucidate the role of the choroidal vasculature in the pathophysiology of RBON by evaluating pRNFL thickness and pCVI in patients with RBON, fellow eyes, and control eyes. Our results showed a decrease in both temporal pRNFL thickness and pCVI in eyes with RBON compared with fellow and control eyes; however, these differences did not reach statistical significance. Although this trend may point to possible structural and vascular involvement in RBON, the lack of statistical significance limits the strength of this interpretation. The observed reduction in temporal pRNFL thickness may indicate the potential involvement of the papillomacular bundle. Nonetheless, the significant decline in BCVA in RBON eyes supports a functional impact on visual acuity, possibly reflecting a combination of inflammatory and microvascular processes.

The function of peripapillary choroidal microvasculature dropout (MvD) in individuals with optic neuritis was examined in a recent study by Lee et al. [11]. According to their research, MvD was more prevalent in the temporal quadrant and was detected in 41.7% of eyes with optic neuritis. Our findings of weakening of the temporal pRNFL in eyes with RBON are comparable to this one. In his study, during the 6-month follow-up, a smaller ganglion cell inner plexiform (GCIP) layer thickness was strongly correlated with the occurrence of MvD. MvD-affected eyes also exhibited reduced temporal quadrant peripapillary retinal vascular density. These results imply that MvD is linked to structural disturbance of the macular GCIP in patients with optic neuritis, which may result in poor visual prognosis. Notably, our results and those of Lee et al. [11] demonstrate how crucial the choroidal vasculature in the pathophysiology of these conditions.

According to a different study by Lee et al. [12], glaucoma and compressive optic neuropathy share MvD, but they present and have different characteristics. In particular, MvD was found in the temporal inferior and superior sectors of the temporal peripapillary sector in glaucoma and compressive optic neuropathy. In addition, MvD development in compressive optic neuropathy was linked to a notable decrease in RNFL thickness and retinal vascular density, which were not observed in glaucoma.

Balci et al. [13] reported a mean macular CVI of 59.6% in affected eyes compared with 61.7% in unaffected eyes in patients with MS who had an optic neuritis attack, suggesting that their attacks may lead to choroidal vascular damage. However, it is important to note that Balci et al found a reduction

https://doi.org/10.5455/annalsmedres.2025.01.02

in macular CVI in affected eyes compared with unaffected fellow eyes, but not in healthy controls.

The fact that MS is commonly associated with optic nerve inflammation [14]. The condition is typically characterized by brain lesions characterized by $CD8^+$ T-cell–mediated inflammatory demyelination [15]. Perivascular accumulations of activated complement proteins and immunoglobulins are typically present within these affected lesions [16] In addition, perivascular infiltration by myelin oligodendrocyte glycoprotein-laden macrophages and $CD4^+$ T cells has also been observed in these lesions [16,17] Numerous OCT-Angio studies have shown reduced macular superficial capillary plexus vessel density in MS patients, suggesting that this may be due to reduced oxygen and metabolite demand secondary to neuroaxonal degeneration and pRFNL and GCIP atrophy [18]. However, other investigators have suggested that MS- or ON-induced inflammation has a direct effect on endothelial dysfunction [19]. Interestingly, previous studies have shown that changes in retinal vascular density share the same characteristics as reduced blood flow in cerebral MS lesions [20,21] This overlap highlights the potential importance of our findings regarding the choroidal vasculature in RBON, as it suggests that the vascular changes we observed may reflect global vascular changes.

One of our study's weaknesses is the small number of patients, which could limit the broad applicability of our findings. Larger cohort studies are necessary in the future to confirm and broaden our findings. In addition, our inability to perform a sectoral analysis of the pCVI is a notable limitation. Incorporating a pretreatment and posttreatment analysis of pCVI could provide valuable insight into the treatment effect on choroidal changes. Future research should consider a sectoral approach to pCVI to identify sector-specific variations indicative of RBON. These steps are critical for advancing our understanding of RBON and may open avenues for novel therapeutic strategies by more thoroughly exploring the vascular aspects of this condition.

CONCLUSION

In conclusion, our study demonstrated a reduction in pCVI and visual acuity in eyes affected by RBON compared with control eyes, supporting the potential role of vascular dysfunction in the disease process. Although reductions in temporal pRNFL thickness and fellow-eye pCVI were observed, these differences did not reach statistical significance. These findings suggest that choroidal vascular alterations, alongside inflammatory mechanisms, may contribute to the pathophysiology of RBON and warrant further investigation in larger cohorts.

Ethics Committee Approval: The research protocol received approval from the Erciyes University Local Ethics Committee (No:2023/39).

Informed Consent: Informed consent was obtained from all individual participants included in the study.

Peer-review: Externally peer-reviewed.

Author Contributions: Concept: H.S.; Design: H.S.; Data Collection and/or Processing: H.S.; Analysis and/or Interpretation: H.K.S.; Literature Review: H.K.S.; Writing: H.S.; Critical Review: H.K.S.

Conflict of Interest: The authors have no conflict of interest to declare.

Financial Disclosure: The authors declared that this study has received no financial support.

REFERENCES

1. Beck RW. The optic neuritis treatment trial: three-year follow-up results. *Arch Ophthalmol.* 1995;113(2):136-137. doi: 10.1001/archopht.1995.01100020014004.
2. Wingerchuk DM, Banwell B, Bennett JL, et al. International consensus diagnostic criteria for neuromyelitis optica spectrum disorders. *Neurology.* 2015;85(2):177-189. doi: 10.1212/wnl.0000000000001729.
3. Balcer LJ. Clinical practice. Optic neuritis. *N Engl J Med.* 2006;354(12):1273-1280. doi: 10.1056/NEJMcp053247.
4. Imamura Y, Fujiwara T, Margolis RON, Spaide RF. Enhanced depth imaging optical coherence tomography of the choroid in central serous chorioretinopathy. *Retina.* 2009;29(10):1469-1473. doi: 10.1097/iae.0b013e3181be0a83.
5. Nickla DL, Wallman J. The multifunctional choroid. *Prog Retin Eye Res.* 2010;29(2):144-168. doi: 10.1016/j.preteyeres.2009.12.002.
6. Park JW, Suh MH, Agrawal R, Khandelwal N. Peripapillary choroidal vascularity index in glaucoma—A comparison between spectral-domain OCT and OCT angiography. *Invest Ophthalmol Vis Sci.* 2018;59(8):3694-3701. doi: 10.1167/iovs.18-24315.
7. Odom JV, Bach M, Brigell M, et al. ISCEV standard for clinical visual evoked potentials:(2016 update). *Doc Ophthalmol.* 2016;133:1-9. doi: 10.1007/s10633-016-9553-y.
8. Agrawal R, Gupta P, Tan KA, Cheung CMG, Wong TY, Cheng CY. Choroidal vascularity index as a measure of vascular status of the choroid: measurements in healthy eyes from a population-based study. *Sci Rep.* 2016;6(1):21090. doi: 10.1038/srep21090.
9. Agrawal R, Salman M, Tan KA, et al. Choroidal vascularity index (CVI)-a novel optical coherence tomography parameter for monitoring patients with panuveitis? *PLoS One.* 2016;11(1):e0146344. doi: 10.1371/journal.pone.0146344.
10. Suh MH, Park JW, Khandelwal N, Agrawal R. Peripapillary choroidal vascularity index and microstructure of parapapillary atrophy. *Invest Ophthalmol Vis Sci.* 2019;60(12):3768-3775. doi: 10.1167/iovs.18-26286.
11. Lee JS, Park S, Kim SS, et al. Peripapillary choroidal microvasculature dropout is associated with poor prognosis in optic neuritis. *PLoS One.* 2023;18(4):e0285017. doi: 10.1371/journal.pone.0285017.
12. Lee EJ, Kim JA, Kim TW, et al. Glaucoma-like parapapillary choroidal microvasculature dropout in patients with compressive optic neuropathy. *Ophthalmology.* 2020;127(12):1652-1662. doi: 10.1016/j.ophtha.2020.06.001.
13. Balci S, Ozcelik Kose A, Yenerel NM. The effect of optic neuritis attacks on choroidal vascularity index in patients with multiple sclerosis. *Graefe's Arch Clin Exp Ophthalmol.* 2021;259:2413-2424. doi: 10.1007/s00417-021-05143-x.
14. Toosy AT, Mason DF, Miller DH. Optic neuritis. *Lancet Neurol.* 2014;13(1):83-99. doi: 10.1016/s1474-4422(13)70259-x.

https://doi.org/10.5455/annalsmedres.2025.01.02

15. Machado-Santos J, Saji E, Tröscher AR, et al. The compartmentalized inflammatory response in the multiple sclerosis brain is composed of tissue-resident $CD8^+$ T lymphocytes and B cells. *Brain.* 2018;141(7):2066-2082. doi: 10.1093/brain/awy151.
16. Takai Y, Misu T, Kaneko K, et al. Myelin oligodendrocyte glycoprotein antibody-associated disease: an immunopathological study. *Brain.* 2020;143(5):1431-1446. doi: 10.1093/brain/awaa102.
17. Marignier R, Hacohen Y, Cobo-Calvo A, et al. Myelin-oligodendrocyte glycoprotein antibody-associated disease. *Lancet Neurol.* 2021;20(9):762-772. doi: 10.1016/s1474-4422(21)00218-0.
18. Mohammadi S, Gouravani M, Salehi MA, et al. Optical coherence tomography angiography measurements in multiple sclerosis: a systematic review and meta-analysis. *J Neuroinflammation.* 2023;20(1):85. doi: 10.1186/s12974-023-02763-4.
19. Murphy OC, Kwakyi O, Iftikhar M, et al. Alterations in the retinal vasculature occur in multiple sclerosis and exhibit novel correlations with disability and visual function measures. *Mult Scler J.* 2020;26(7):815-828. doi: 10.1177/1352458519845116.
20. Paling D, Thade Petersen E, Tozer DJ, et al. Cerebral arterial bolus arrival time is prolonged in multiple sclerosis and associated with disability. *J Cereb Blood Flow Metab.* 2014;34(1):34-42. doi: 10.1038/jcbfm.2013.161.
21. Inglese M, Adhya S, Johnson G, et al. Perfusion magnetic resonance imaging correlates of neuropsychological impairment in multiple sclerosis. *J Cereb Blood Flow Metab*. 2008;28(1):164-171. doi: 10.1038/sj.jcbfm.9600504.

https://doi.org/10.5455/annalsmedres.2025.01.02